Electronic Supplementary Information

Non-covalent polyhedral oligomeric silsesquioxane-polyoxometalates as inorganic–organic–inorganic hybrid materials for visible-light photocatalytic splitting of water

Rajendran Prabu,[1,2,#] Peramaiah Karthik,[2,#] Nallasamy Palanisami,[3] Paolo P. Pescarmona,[4] Bernaurdshaw Neppolian[2] and Swaminathan Shanmugan[1,2,*]

[1]Department of Chemistry, SRM Institute of Science and Technology, Kattankulathur, Kancheepuram 603203, Tamil Nadu, India.

[2]SRM Research Institute, SRM Institute of Science and Technology, Kattankulathur, Kancheepuram 603203, Tamil Nadu, India.

[3]Department of Chemistry, School of Advanced Sciences, VIT University, Vellore 632014, Tamil Nadu, India.

[4]Chemical Engineering Group, Engineering and Technology institute Groningen (ENTEG), University of Groningen, Nijenborgh 4, 9747AG Groningen, The Netherlands.

# Authors contributed equally

Corresponding author: Swaminathan Shanmugan (shanmugan.s@ktr.srmuniv.ac.in)

Contents

Figure S10. UV-vis absorbance spectra of free POMs in water (Reaction solution).

Figure S11. Mott-Schottky plots for POSS-NH_2.

Table S3. Comparison of hydrogen production for POM based materials.

Section S1

Synthesis of heptaisobutylpropylamine-T8-Silsesquioxane (POSS-NH_2):

To a solution of 1,3,5,7,9,11,14-Heptaisobutyl tricyclo[7.3.3.1]heptasiloxane-endo-3,7,14-triol (2 g, 2.53 mmol) in dichloromethane (20 mL), (3-Aminopropyl) trimethoxysilane (0.5 ml, 2.79 mmol) in dichloromethane (20 mL) was added under nitrogen atmosphere at RT. The reaction mixture was stirred for 48 hours, then the colourless solution was evaporated under vacuum to afford colourless solid (POSS-NH_2). Yield: 2.23g (89%). IR (KBr, cm^{-1}): 3390(br), 2955(s), 1579(br), 1465(m), 1332(w), 1231(m), 1113(s), 956(m), 837(m), 745(s), 687(w), 560(w), 482(m). ^1H NMR (500 MHz, $CDCl_3$, TMS, ppm): δ= 0.58 (t, 2H, -$\mathit{CH_2}CH_2CH_2NH_2$), 0.60(d, 14H,-$CH_2$ in ^{i}Bu), 0.95 (dd, 42H,-CH_3), 1.55 (m, 2H, -$CH_2\mathit{CH_2}CH_2NH_2$), 1.85 (septet, 7H, -CH), 2.67 (t, 2H, -$CH_2CH_2\mathit{CH_2}NH_2$). ^{13}C NMR (100 MHz, $CDCl_3$, TMS, ppm): δ= 44.9, 27.3, 25.8, 24.0, 22.6, and 9.3 (aliphatic-carbons). ^{29}Si NMR (79.30 MHz, $CDCl_3$, TMS, ppm): δ= -67.8, -67.6, -67.2. Positive ion ESI-Mass m/z = 874.20 [POSS-NH_2].

Photo-electrochemical studies

The conventional three-electrode system was used for the photo-electrochemical studies. Saturated Ag/AgCl and Pt wire were used as reference and counter electrodes, respectively. For the photocurrent measurement, 250 W Xe arc lamp (OSRAM, Germany) was utilized as a light source. The working electrode was prepared by the mixing 50 mg of photocatalyst with 150 ml of PEG (mol. Wt 400) and 125 ml of ethanol. Then, it was coated on a 2.5 cm^2 fluorine-doped tin oxide (FTO) glass substrate with an active area of about 1 cm^2 by a doctor-blade method using scotch tape as the spacer and it was dried at 80 ^oC.[1]

Description of the photoluminescence (PL) emission measurements

We have performed PL analysis in solid state mode. The synthesized POM-POSS hybrid materials were loaded in a sample holder and the PL emission spectra were recorded using a spectrofluorometer (Fluoramax4p) at 250 nm excitation wavelength. Importantly, the excitation wavelength was kept constant for all the measurements. The excitation wavelength of the POSS-NH_2 was chosen based on the UV-DRS absorbance spectra (Fig. 5). It was clearly seen that the absorption edge of POSS-NH_2 is located at ~ 250 nm.

Table S1. Solubility of POMs, POSS-NH_2 and POM-POSS Materials

SOLVENT	**$H_3PW_{12}O_{40}$**	**$H_3PMo_{12}O_{40}$**	**$H_5V_2Mo_{10}O_{40}$**	**POSS-NH_2**	**POM(W)-POSS**	**POM(Mo)-POSS**	**POSS(MoV)-POSS**
WATER	Soluble	Soluble	Soluble	Insoluble	Insoluble	Insoluble	Insoluble
ETHANOL	Soluble	Soluble	Soluble	Soluble	Insoluble	Insoluble	Insoluble
METHANOL	Soluble	Soluble	Soluble	Insoluble	Soluble	Soluble	Soluble
TETRAHYDROFURAN	Insoluble	Insoluble	Insoluble	Soluble	Soluble	Soluble	Soluble
DICHLOROMETHANE	Insoluble	Insoluble	Insoluble	Soluble	Soluble	Soluble	Soluble
HEXANE	Insoluble	Insoluble	Insoluble	Soluble	Soluble	Soluble	Soluble

Table S2. ^{1}H NMR Integral values of POSS-NH_2, POM(W)-POSS, POM(Mo)-POSS and POM(MoV)-POSS.

Compounds	**Peaks**	**δ-value (ppm)**	**Integral value**	**Ratio**
POSS-NH_2	$-CH_2CH_2\mathbf{CH_2}NH_2$	2.67	1	1:1:8:21:3.5 (1 ^{n}Pr : 7 ^{i}Bu)
	$-CH_2\mathbf{CH_2}CH_2NH_2$	1.55	0.9	
	$-\mathbf{CH_2}CH_2CH_2NH_2$ & $-\mathbf{CH_2}$ in ^{i}Bu	0.58 & 0.60	8.4	
	$-\mathbf{CH_3}$ in ^{i}Bu	0.95	21.4	
	$-\mathbf{CH}$ in ^{i}Bu	1.85	3.9	
POM(W)-POSS	$-CH_2CH_2\mathbf{CH_2}NH_2$	3.31	1	1:1:8:21:3.5 (1 ^{n}Pr : 7 ^{i}Bu for each cage)
	$-CH_2\mathbf{CH_2}CH_2NH_2$	1.25	0.8	
	$-\mathbf{CH_2}CH_2CH_2NH_2$ & $-\mathbf{CH_2}$ in ^{i}Bu	0.58 & 0.60	8.6	
	$-\mathbf{CH_3}$ in ^{i}Bu	0.95	21.3	
	$-\mathbf{CH}$ in ^{i}Bu	1.85	3.7	
POM(Mo)-POSS	$-CH_2CH_2\mathbf{CH_2}NH_2$	3.36	1	1:1:8:21:3.5 (1 ^{n}Pr : 7 ^{i}Bu for each cage)
	$-CH_2\mathbf{CH_2}CH_2NH_2$	1.25	0.9	
	$-\mathbf{CH_2}CH_2CH_2NH_2$ & $-\mathbf{CH_2}$ in ^{i}Bu	0.58 & 0.60	8.2	
	$-\mathbf{CH_3}$ in ^{i}Bu	0.95	21.4	
	$-\mathbf{CH}$ in ^{i}Bu	1.85	3.1	
POM(MoV)-POSS	$-CH_2CH_2\mathbf{CH_2}NH_2$	2.96	1	1:1:8:21:3.5 (1 ^{n}Pr : 7 ^{i}Bu for each cage)
	$-CH_2\mathbf{CH_2}CH_2NH_2$	1.25	0.8	
	$-\mathbf{CH_2}CH_2CH_2NH_2$ & $-\mathbf{CH_2}$ in ^{i}Bu	0.58 & 0.60	8.1	
	$-\mathbf{CH_3}$ in ^{i}Bu	0.95	21.2	
	$-\mathbf{CH}$ in ^{i}Bu	1.85	3.3	

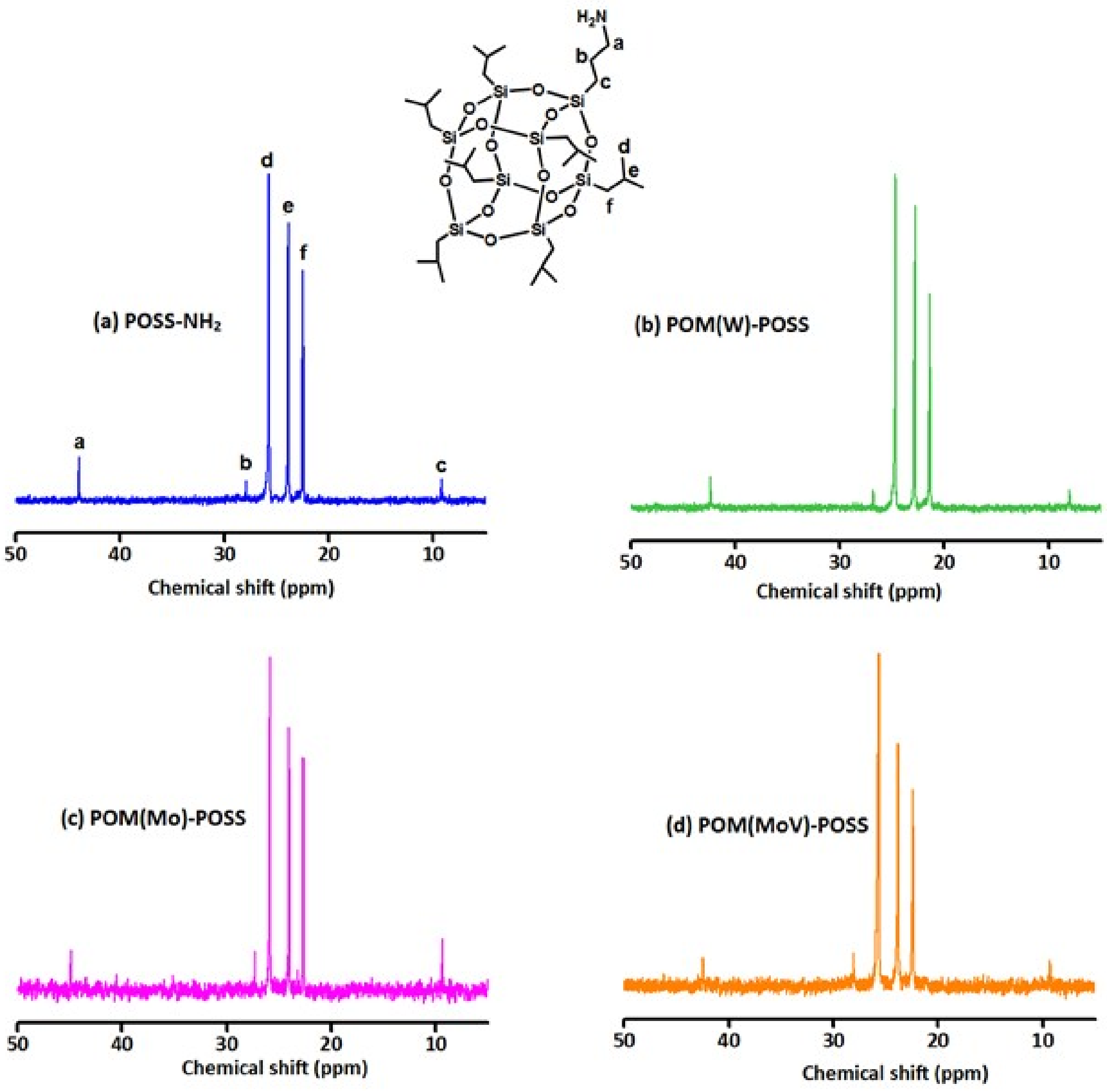

Fig. S1 ^{13}C NMR spectra of POSS-NH$_2$, POM(W)-POSS, POM(Mo)-POSS and POM(MoV)-POSS in CDCl$_3$.

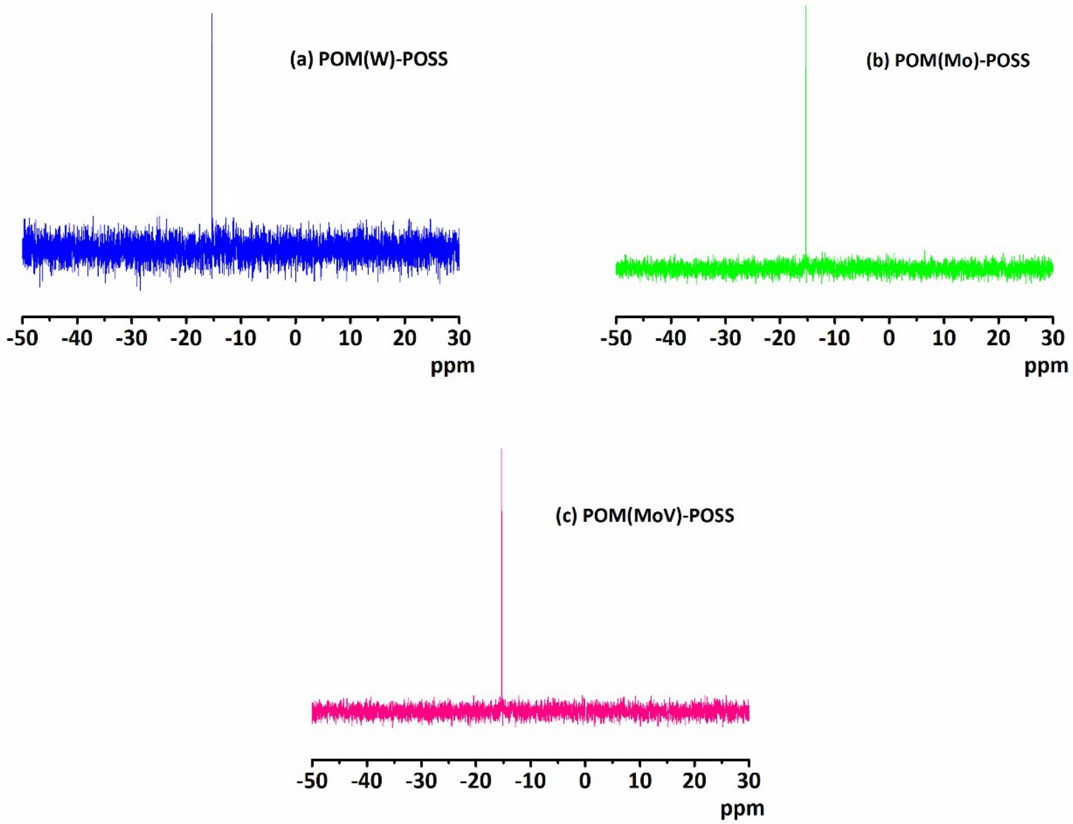

Fig. S2 ^{31}P NMR spectra of POM(W)-POSS, POM(Mo)-POSS and POM(MoV)-POSS in $CDCl_3$.

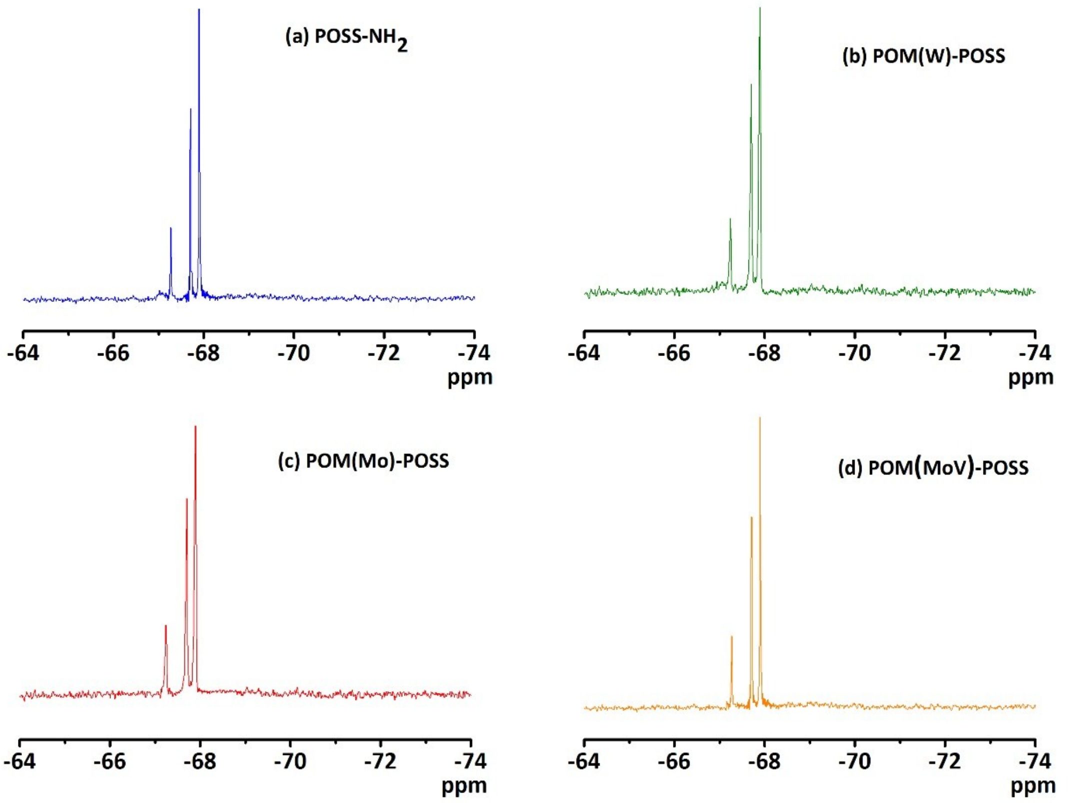

Fig. S3 ^{29}Si NMR spectra of POSS-NH$_2$, POM(W)-POSS, POM(Mo)-POSS and POM(MoV)-POSS in CDCl$_3$.

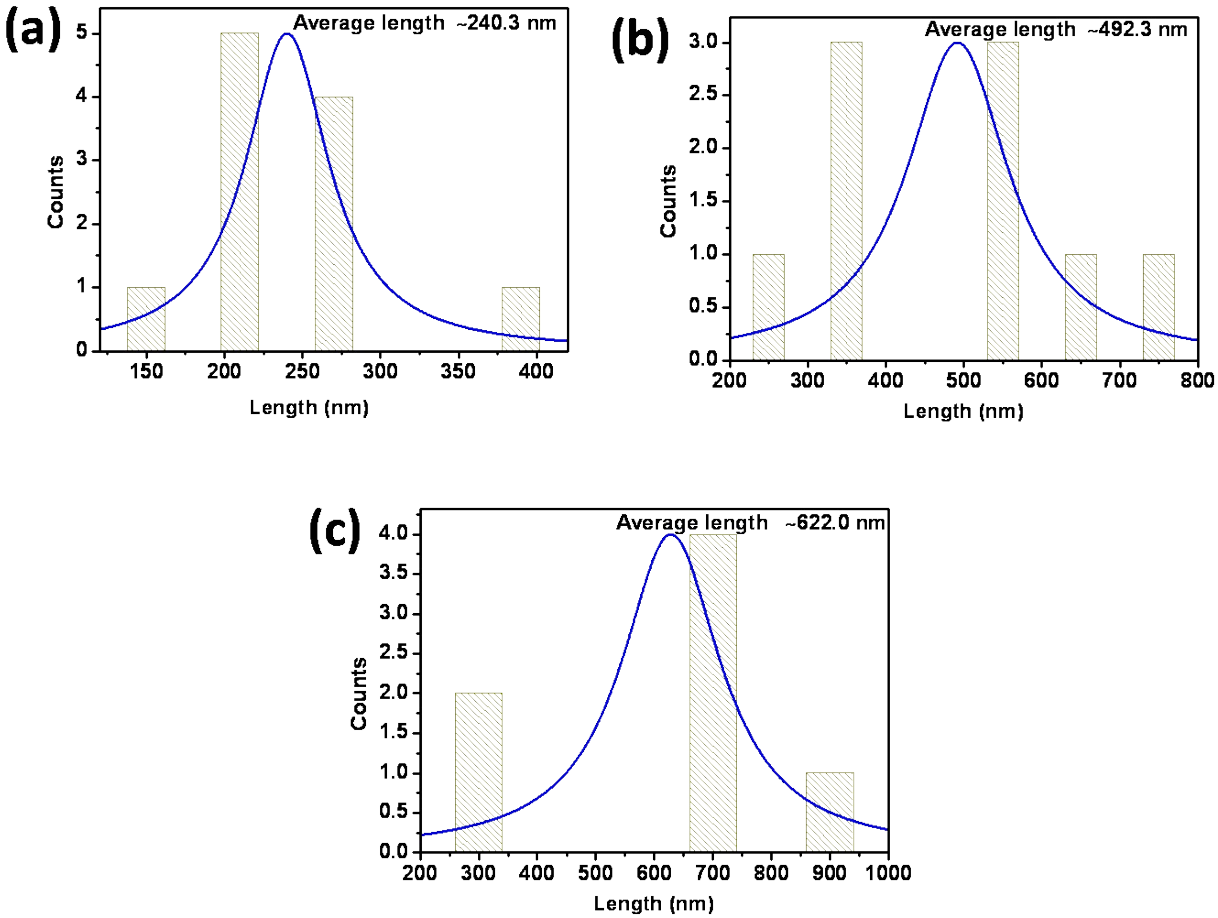

Fig. S4 Particle size distribution analysis: (a) POM(W)-POSS; (b) POM(Mo)-POSS; (c) POM(MoV)-POSS.

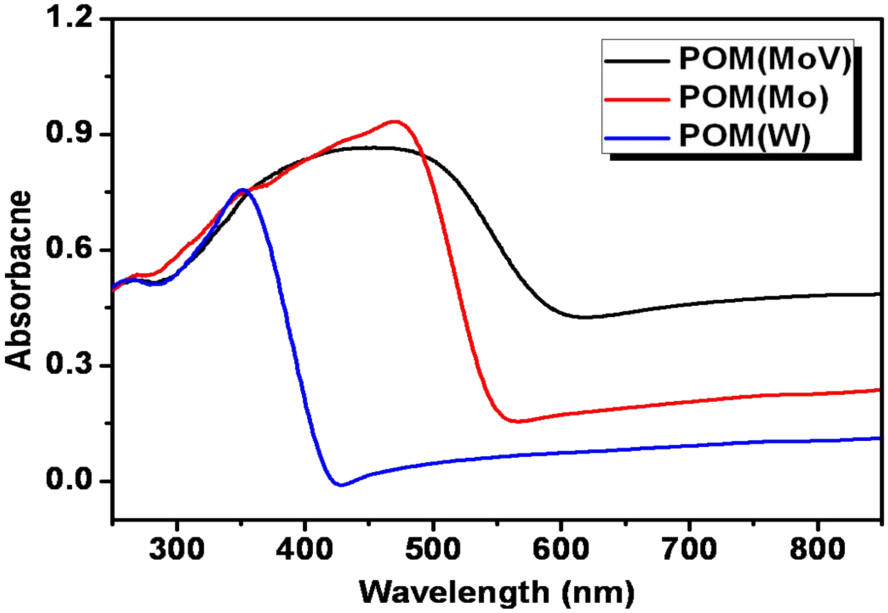

Fig. S5 UV-vis DRS spectra of free POMs

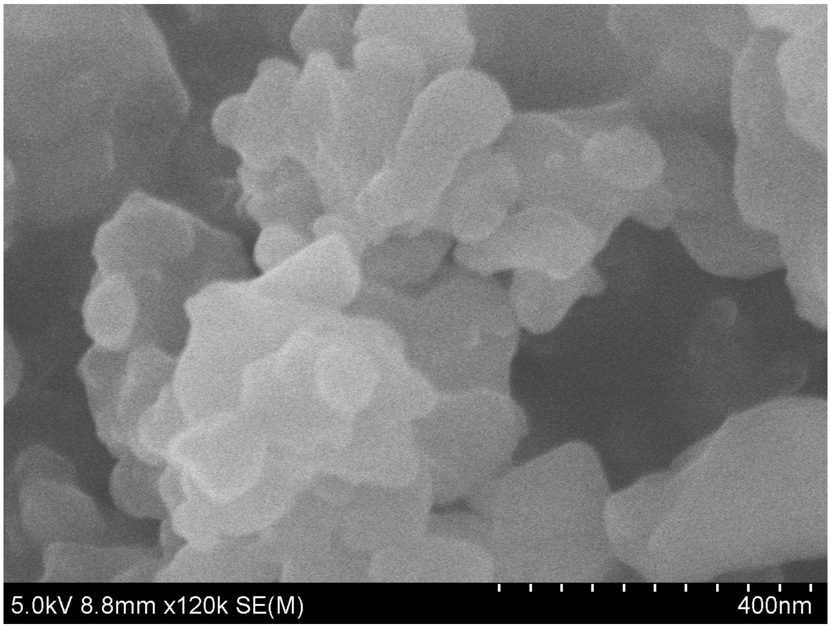

Fig. S6 SEM Image of POM(MoV)-POSS hybrids after 5 cycles of photocatalytic H_2 production reaction.

In order to compare the photocatalytic H_2 production activity of POMs with POSS-NH_2 hybrids, we have performed photocatalytic H_2 production experiments for pristine POMs. It is very interesting to point out that the pristine POMs did not show any H_2 production activity under similar conditions (Fig. S7, S8 and S9). This can be explained considering that the high solubility of POMs in water makes them unstable and thereby restrict their photocatalytic activity. A similar result was previously reported by Zhou et. al for photocatalytic degradation of Rhodamine B by using molybdenum–based polyoxometalates.[2] Theyconcluded that during photocatalysis process, the POMs decomposed due to high anionic charge.[2,3] Moreover, the instability of POMs in the reaction solution was confirmed by UV-vis absorbance spectroscopy. As shown in Fig. S10, there is no characteristic absorption peak observed in the visible region for free POMs in water. This result clearly confirms the instability of POMs in water and it also reflected in their photocatalytic activity.

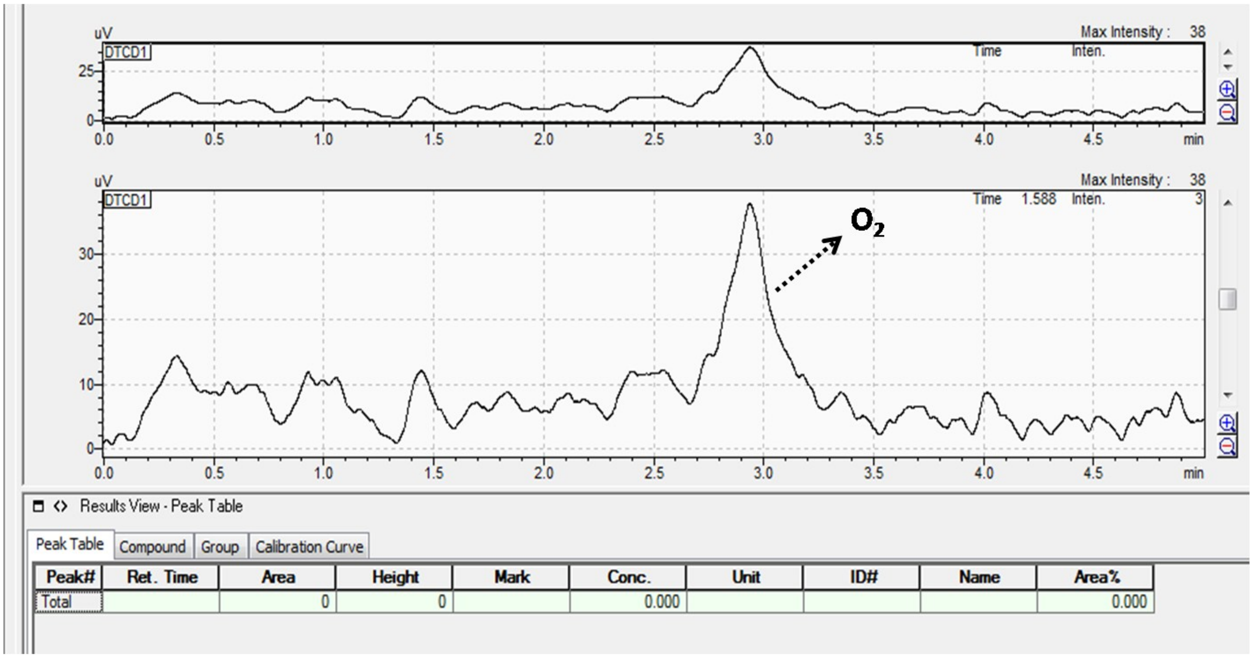

Peak#	Ret. Time	Area	Height	Mark	Conc.	Unit	ID#	Name	Area%
Total		0	0		0.000				0.000

Fig. S7 GC graph of photocatalytic H_2 production using free POM(MoV).

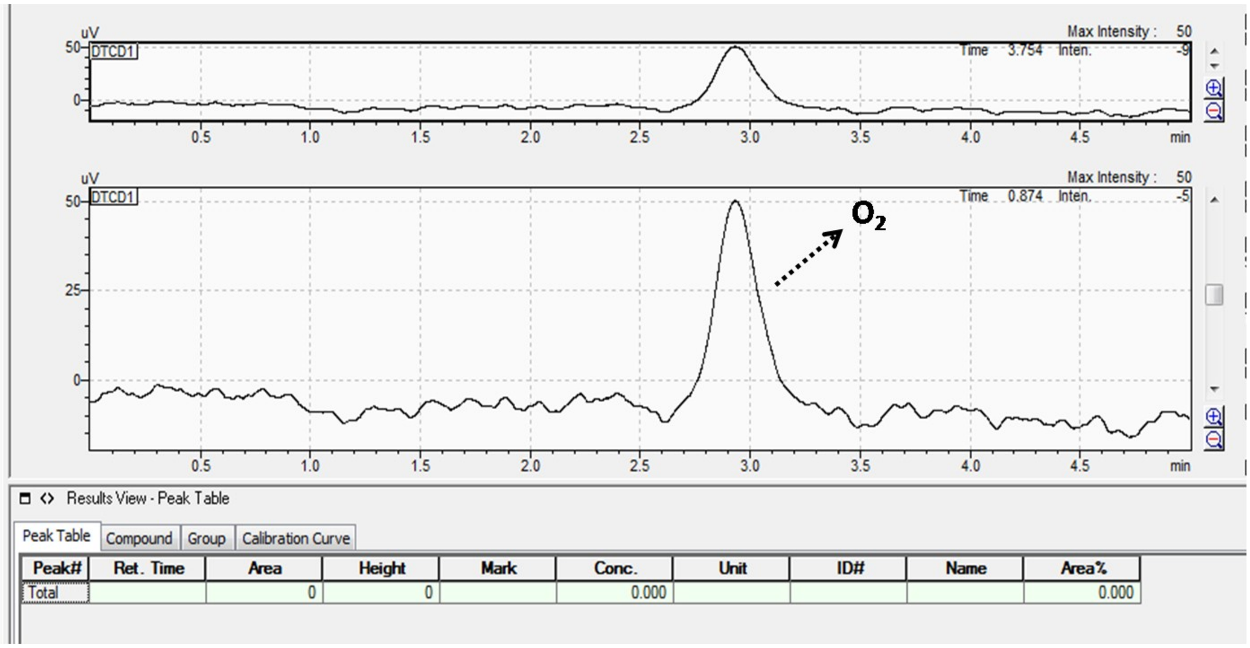

Peak#	Ret. Time	Area	Height	Mark	Conc.	Unit	ID#	Name	Area%
Total		0	0		0.000				0.000

Fig. S8 GC graph of photocatalytic H_2 production using free POM(Mo).

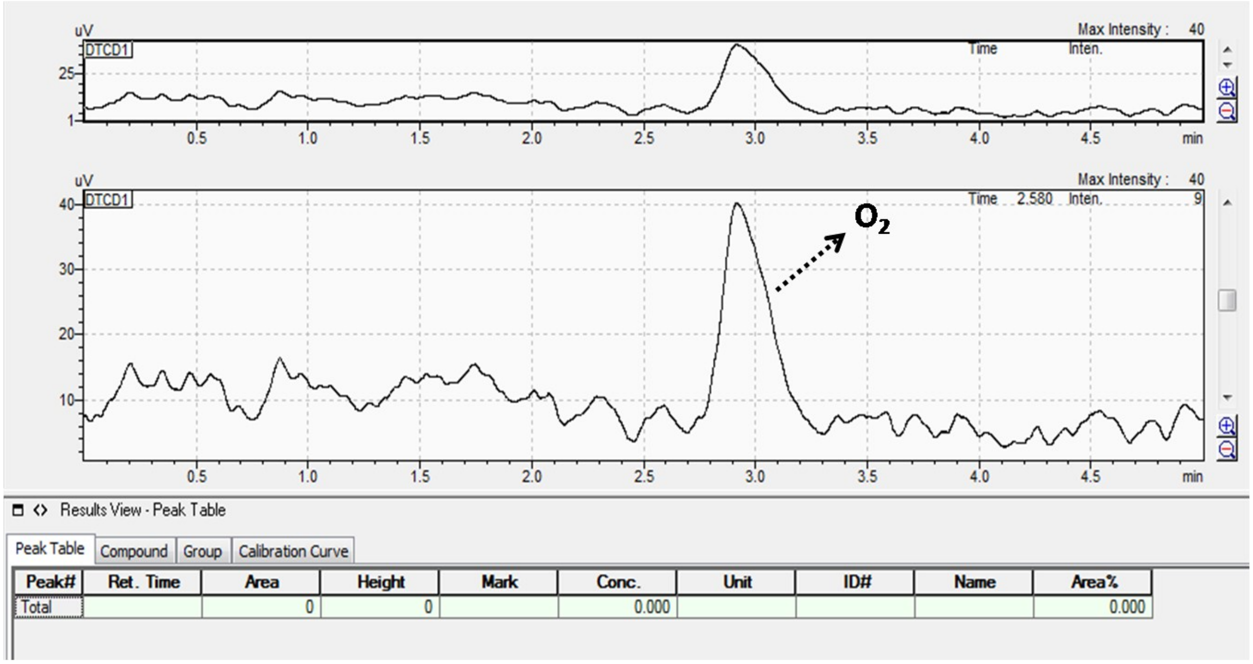

Peak#	Ret. Time	Area	Height	Mark	Conc.	Unit	ID#	Name	Area%
Total		0	0		0.000				0.000

Fig. S9 GC graph of photocatalytic H_2 production using free POM(W).

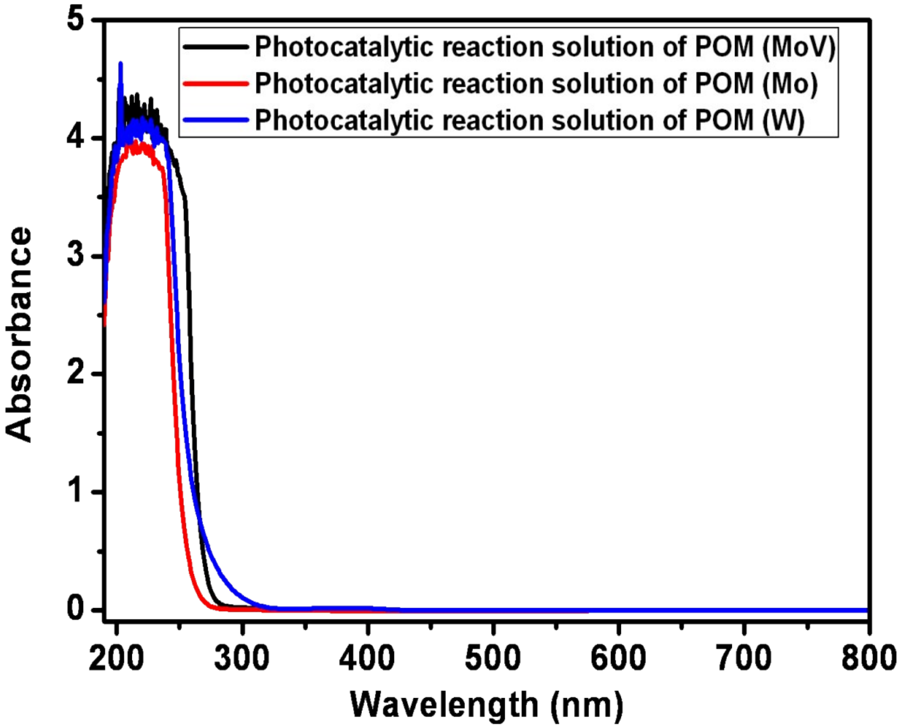

Fig. S10 UV-vis absorbance spectra of free POMs in water (reaction solution).

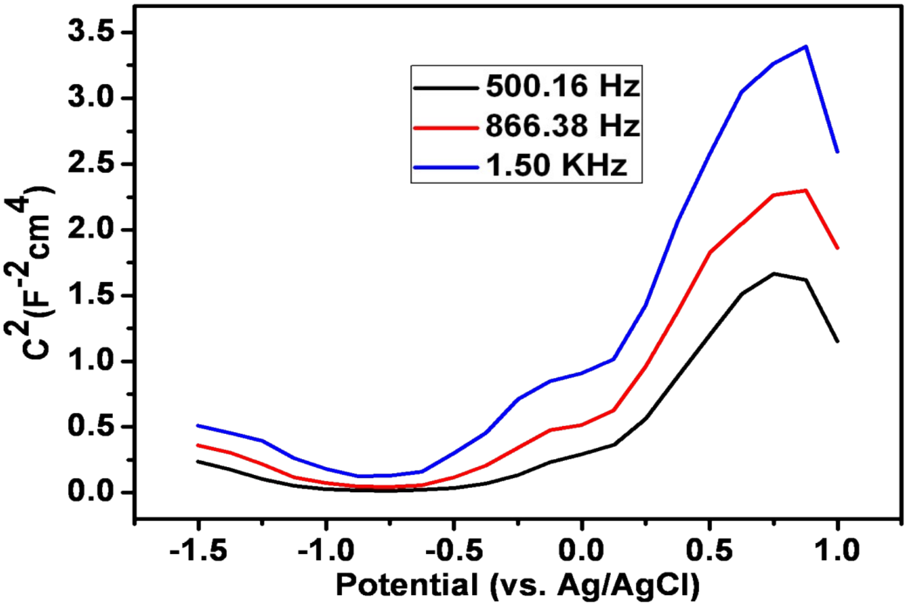

Fig. S11 Mott-Schottky plots for POSS-NH_2.

The charge carrier densities (ND) of POSS-NH_2 and POSS-POMs hybrids were calculated by using following equation:

$$ND = 2/(e\varepsilon\varepsilon_0 m)$$

From the linear portion of the Mott–Schottky plots (Fig. S11 and Fig. 8), the slope values (m) corresponding to POSS-NH_2, POM(W)-POSS, POM(Mo)-POSS and POM(MoV)-POSS were found to be 1.25, 3×10^{-3}, 2.1×10^{-2} and 1.6×10^{-2} respectively. These results clearly indicate that integration of double metal site POM with POSS facilitates charge transport in line with PL studies and the enhanced photocatalytic H_2 production activity.

Table S3. Comparison of hydrogen production for POM based materials

S.No.	Catalyst name	Reaction condition	Co-catalyst	Amount of H_2 produced	pH	ref
1	POM(MoV)-POSS	Light source: 300 W Xe lamp, Sacrificial agent: TEOA Light intensity: 200mW/cm^2	Nil	485 µmol g^{-1} h^{-1}	11.21	This work
2	POM(Mo)-POSS	Light source: 300 W Xe lamp, Sacrificial agent: TEOA Light intensity: 200mW/cm^2	Nil	371 µmol g^{-1} h^{-1}	11.8	
3	POM(W)-POSS	Light source: 300 W Xe lamp, Sacrificial agent: TEOA Light intensity: 200mW/cm^2	Nil	302 µmol g^{-1}h^{-1}	12.41	
4.	$(HTEA)_2\{[Na(TEA)_2]H[SiW_{12}O_{40}]\}\cdot 5H_2O$	Light source: 300 W Xe lamp, Sacrificial agent: CH_3OH Light intensity: n.a.	Pt	7.435 µmol g^{-1} h^{-1}	Nil	4
5.	$(HTEA)_2\{[Na(TEA)_2][PW_{12}O_{40}]\}\cdot 4H_2O$	Light source: 300 W Xe lamp Sacrificial agent: CH_3OH Light intensity: n.a.	Pt	7.838 µmolg^{-1} h^{-1}		
6.	$(HTEA)_2\{[Na(TEA)_2]H[GeW_{12}O_{40}]\}\cdot 4H_2O$	Light source: 300 W Xe lamp Sacrificial agent: CH_3OH Light intensity: n.a.	Pt	7.375 µmol g^{-1} h^{-1}		
7.	$[Cu(en)_2]_4[PNb_{12}O_{40}(VO)_6].(OH)_5.8H_2O$	Light source: 125W Hg lamp Sacrificial agent: CH_3OH Light intensity: n.a.	Pt	44.35 mol g^{-1} h^{-1}		

8.	$[Cu(en)_2]_4[PNb_{12}O_{40}(VO)_6].(OH)_5.8H_2O$	Light source: 300 W Xe lamp Sacrificial agent**:** CH_3OH Light intensity**:** n.a.	Pt	10.31 mmol g^{-1} h^{-1}	Nil	5
9.	$[Cu(enMe)_2]_4[PNb_{12}O_{40}(VO)_6].(OH)_5.6H_2O$	Light source: 125W Hg lamp Sacrificial agent**:** CH_3OH Light intensity**:** n.a.	Pt	43.86 mmol g^{-1} h^{-1}		
10.	$[Cu(enMe)_2]_4[PNb_{12}O_{40}(VO)_6].(OH)_5.6H_2O$	Light source: 300 W Xe lamp Sacrificial agent**:** CH_3OH Light intensity**:** 200mW/cm^2	Pt	10.45 mmol g^{-1} h^{-1}		
11.	$[Cu(en)_2]_{11}K_4Na_2[KNb_{24}O_{72}H_9]_2\cdot 120H_2O$	Light source: 500 W Xe lamp. Sacrificial agent**:** TEA Light intensity**:** n.a.	(CoIII(dmgH)$^{2-}$ pyCl	13.2 μmol g^{-1} h^{-1}	Nil	6
12.	$[Cu(en)_2]_{11}K_4Na_2[KNb_{24}O_{72}H_9]_2\cdot 120H_2O$	Light source: 125 W mercury lamp Sacrificial agent**:** TEA Light intensity**:** n.a.	(CoIII(dmgH)$^{2-}$ pyCl	1000 μmol h^{-1} g^{-1}		
13.	$K_{10}[Nb_2O_2(H_2O)_2]$-$[SiNb_{12}O_{40}]_3$ $12H_2O$	Light source: 300 W Xe lamp Sacrificial agent**:** CH_3OH Light intensity**:** n.a.	Pt	2100 μmol h^{-1} g^{-1}	Nil	7
14.	$K_{10}[Nb_2O_2(H_2O)_2]$-$[SiNb_{12}O_{40}]_3$ $12H_2O$	Light source:300 W Xe lamp pure water. Light intensity**:** 200mW/cm^2	NiO	222 μmol h^{-1} g^{-1}		
15.	$K_7[Co^{III}Co^{II}(H_2O)W_{11}O_{39}]$	Light source: 3 W LED lamp Sacrificial agent: TEOA/H_2O Light intensity**:** n.a.	Pt	13395 μmol h^{-1} g^{-1}	7.0	8
16.	$(NH_4)7H[ZnCo^{II}(H_2O)W_{11}O_{39}]$	Light source: 3 W LED lamp Sacrificial agent:TEOA/H_2O Light intensity**:** n.a.	Pt	5301 μmolh^{-1} g^{-1}		

17.	$K_6[SiCo^{II}(H_2O)W_{11}O_{39}]$	Light source: 3 W LED lamp Sacrificial agent:TEOA/H_2O Light intensity: n.a.	Pt	4614 µmol h^{-1} g^{-1}		
18.	$K_5[PCo^{II}(H_2O)W_{11}O_{39}]$	Light source: 3 W LED lamp Sacrificial agent: TEOA/H_2O Light intensity: n.a.	Pt	5157 µmol h^{-1} g^{-1}		
19.	$K_5[Co^{III}W_{12}O_{40}]$	Light source: 3 W LED lamp Sacrificial agent: TEOA/H_2O Light intensity: n.a.	Pt	4579 µmolh^{-1} g^{-1}		
20.	$Na_3PW_{12}O_{40}$	Light source: 3 W LED lamp Sacrificial agent:TEOA/H_2O Light intensity: n.a.	Pt	0 µmol h^{-1} g^{-1}		
21.	$Rb_8K_2[\{Ru_4O_4(OH)_2(H_2O)_4\}$-(g-$SiW_{10}O_{36})_2]$	Light source: Xe lamp, 420–520 nm Sacrificial agent: [Ru(bpy)3]$^{2+}$ Light intensity: n.a.	Nil	TON 8 x10^{-2} s^{-1}	7.2	9
22.	$Cs_9[(gPW_{10}O_{36})_2Ru^{IV}{}_4O_5(OH)(OH_2)_4]$	Light source: Xe lamp (420–520 nm), Sacrificial agent: $[Ru(bpy)_3]Cl_2$ Light intensity: n.a.	Nil	TOF 0.13 s^{-1}	5.8	10

References:

1. S. G. Babu, R. Vinoth, D. P. Kumar, M. V. Shankar, H.-L. Chou, K. Vinodgopal and B. Neppolian, *Nanoscale*, 2015, **7**, 7849-7857.
2. Y. Zhou, L. Qin, C. Yu, T. Xiong, L. Zhang, W. Ahmad and H. Han, *RSC Adv.,* 2014, **4**, 54928-54935.
3. A. Müller, E. Krickemeyer, H. Bögge, M. Schmidtmann and F. Peters, *Angew. Chem., Int. Ed.,,* 1998, **37**, 3359-3363.
4. Y. Nie, W. Chen, Z. Liu and E. Wang, *Inorg. Chem. Commun.*, 2015, **61**, 184-186.
5. J.-Q. Shen, Y. Zhang, Z.-M. Zhang, Y.-G. Li, Y.-Q. Gao and E.-B. Wang, *Chem. Commun.*, 2014, **50**, 6017-6019.
6. Z.-L. Wang, H.-Q. Tan, W.-L. Chen, Y.-G. Li and E.-B. Wang, *Dalton Trans.*, 2012, **41**, 9882-9884.
7. Z. Zhang, Q. Lin, D. Kurunthu, T. Wu, F. Zuo, S.-T. Zheng, C. J. Bardeen, X. Bu and P. Feng, *J. Am. Chem. Soc.*, 2011, **133**, 6934-6937.
8. J. Zhao, Y. Ding, J. Wei, X. Du, Y. Yu and R. Han, *Int. J. Hydrog. Energy*, 2014, **39**, 18908-18918.
9. F. Puntoriero, G. La Ganga, A. Sartorel, M. Carraro, G. Scorrano, M. Bonchio and S. Campagna, *Chem. Commun.*, 2010, **46**, 4725-4727.
10. C. Besson, Z. Huang, Y. V. Geletii, S. Lense, K. I. Hardcastle, D. G. Musaev, T. Lian, A. Proust and C. L. Hill, *Chem. Commun.*, 2010, **46**, 2784-2786.